Crystal Structure of the Catalytic Subunit of cAMP-Dependent Protein Kinase Complexed with MgATP and Peptide Inhibitor[†,‡]

Jianhua Zheng,[§] Daniel R. Knighton,[§,∥] Lynn F. Ten Eyck,[§,⊥] Rolf Karlsson,[∥] Nguyen-huu Xuong,[§,#,△] Susan S. Taylor,[§] and Janusz M. Sowadski[*,∥,#]

Departments of Chemistry, Biology, Physics, and Medicine, University of California at San Diego, 9500 Gilman Drive, La Jolla, California 92093, and San Diego Supercomputer Center, P.O. Box 85608, San Diego, California 92186

Received October 22, 1992; Revised Manuscript Received December 17, 1992

ABSTRACT: The structure of a ternary complex of the catalytic subunit of cAMP-dependent protein kinase, MgATP, and a 20-residue inhibitor peptide was determined at a resolution of 2.7 Å using the difference Fourier technique starting from the model of the binary complex (Knighton et al., 1991a). The model of the ternary complex was refined using both X-PLOR and TNT to an *R* factor of 0.212 and 0.224, respectively. The orientation of the nucleotide and the interactions of MgATP with numerous conserved residues at the active site of the enzyme are clearly defined. The unique protein kinase nucleotide binding site consists of a five-stranded antiparallel β-sheet with the base buried in a hydrophobic site along β-strands 1 and 2 and fixed by hydrogen bonds to the N6 amino and N7 nitrogens. The small lobe secures the nucleotide via a glycine-rich loop and by ion pairing with Lys72 and Glu91. While the small lobe fixes the nontransferable α- and β-phosphates in this inhibitor complex, the γ-phosphate is secured by two Mg^{2+} ions and interacts both directly and indirectly with several residues in the large lobe—Asp184, Asn171, Lys168. Asp166 is positioned to serve as a catalytic base. The structure is correlated with previous chemical evidence, and the features that distinguish this nucleotide binding motif from other nucleotide binding proteins are delineated.

Protein kinases constitute a large and diverse family of enzymes. One of the simplest members of this family is the catalytic (C) subunit of cyclic adenosine monophosphate (cAMP) dependent protein kinase (cAPK) (Taylor et al., 1990a). cAPK was one of the first protein kinases to be discovered and purified (Walsh et al., 1968). It was the first to be sequenced (Shoji et al., 1979) and the first to be cloned and expressed in large quantities in *Escherichia coli* (Slice & Taylor, 1989). Its simplicity derives not only from its size (350 residues) but also from its unique mechanism of activation. In the absence of cAMP, the enzyme is sequestered as an inactive tetrameric complex containing both regulatory (R) and catalytic subunits. Upon binding of cAMP, the holoenzyme (R_2C_2) dissociates into an R_2–$cAMP_4$ dimer and two active, monomeric C subunits. Although the protein kinase family is both large and structurally diverse, all of the eukaryotic protein kinases share a conserved catalytic core, and this core is contained within the C subunit (Hanks et al., 1988).

Because of its simplicity, relative abundance, and ease of purification, the C subunit has served as a framework for this entire family of enzymes. Essential residues, many identified initially using biochemical techniques, are found to be invariant throughout the family. Recently, a crystal structure of the C subunit was solved at a resolution of 2.7 Å (Knighton et al., 1991a,b). This structure is of a binary complex containing the C subunit and a high-affinity 20-residue inhibitor peptide derived from the amino terminal portion of a naturally occurring heat-stable protein kinase inhibitor (PKI). It not only represents the first protein kinase structure to be solved but also provides a three-dimensional structure of the bound inhibitor peptide and its interactions with the protein.

The ATP binding site of the C subunit has been probed using a variety of approaches. Chemical modifications, including both affinity labeling and group-specific labeling, have identified specific amino acids that contribute to the binding of MgATP (for a review, see Taylor et al. (1990a)). Affinity labeling, for example, placed Lys72 at the ATP binding site (Zoller et al., 1981), while differential labeling with acetic anhydride provided a more general profile of the MgATP binding site and its location near the N-terminus (Buechler et al., 1989). Differential labeling with a hydrophobic carbodiimide placed Asp184 and Glu91 near the ATP binding site (Buechler & Taylor, 1988) and demonstrated, furthermore, that Asp184 could cross-link to Lys72 (Buechler & Taylor, 1989). The ATP binding site also was mapped with analogs, both as a free enzyme (Flockhart et al., 1980) and as a type I holoenzyme complex where MgATP binds with a high affinity (Hoppe et al., 1978). NMR also was used to elucidate the structural features of the bound nucleotide.

The structure of the binary complex defines the general topology of the enzyme, localizes the essential residues, and forms a template for the folding of the catalytic core in all protein kinases. However, in order to fully understand the functioning of this enzyme, it is essential not only to view the binary complex but also to compare the binary complex with a ternary complex containing magnesium adenosine triphosphate (MgATP) and evenutally with the apoenzyme containing no bound substrates or inhibitors. We report here

[†] Supported by the Lucille P. Markey Charitable Trust, without which this work could not have been completed, by grants from NIH (S.S.T., N.-h.X., and J.M.S.), the American Cancer Society (J.M.S. and S.S.T.), and NSF (S.S.T. and L.T.E.), by NIH training grants T32CA09523 and T32DK07233 (D.R.K.), and by the University of California (J.M.S.).

[‡] The coordinates for a 2.0-Å binary complex are available from the Brookhaven Protein Data Bank as entry 1APM. The coordinates for the ternary complex are available from the Brookhaven Protein Data Bank as entry 1ATP. These coordinates reflect a 2.2-Å refinement completed after the submission of this manuscript.

* Author to whom correspondence should be addressed.
[§] Department of Chemistry.
[∥] Department of Medicine.
[⊥] San Diego Supercomputer Center.
[#] Department of Biology.
[△] Department of Physics.

0006-2960/93/0432-2154$04.00/0

Table I: Diffraction Data

crystals	resolution (Å)	reflections	completeness (%)	R_{sym}
high [Mg^{2+}]	2.7	12 614	90.5	0.041
low [Mg^{2+}]	2.7	12 010	92.1	0.058

the structure of a ternary complex containing the C subunit, an inhibitor peptide PKI(5-24), and MgATP. This ternary complex allows us to understand more fully why many of the conserved residues at the active site are important for function.

EXPERIMENTAL PROCEDURES

Proteins and Peptides. The mouse Cα subunit was expressed in *E. coli* and purified by phosphocellulose chromatography followed by gel filtration as described previously (Yonemoto et al., 1991). The inhibitor peptide corresponding to the amino terminal region of PKI was synthesized by Advanced Chem Tech (Louisville, KY) and purified to homogeneity by high-performance liquid chromatography. The peptide constitutes the major inhibitory segment of PKI and has an apparent K_i of 2 nM (Walsh et al., 1990).

Crystallization. The C subunit was crystallized as a ternary complex using enzyme/inhibitor/Mg^{2+}/ATP molar ratios of 1:3:5:20. Crystals of the recombinant mouse C subunit complexes with MgATP and PKI(5-24) were grown according to Zheng et al. (1991, 1992). The C subunit was brought to a final concentration of 10 mg/mL and dialyzed against 50 mM bicine buffer (pH 8.0) and 150 mM ammonium acetate. Crystals were grown at 4 °C by hanging drop vapor diffusion. The reservoir contained 10 mM dithiothreitol (DTT) and 8% (w/v) poly(ethylene glycol) 400. The drop contained equal volumes of protein solution, reservoir solution without methanol, and 10 mM DTT solution containing PKI(5-24) and MgATP. Methanol was added to the reservoir solution of a concentration of 15% before the cover slip was sealed. Two types of ternary crystals were examined: one grown in a solution containing 0.44 mM $MgCl_2$ (low-[Mg^{2+}] crystals), as described above, and the other grown in 0.44 mM $MgCl_2$ and then soaked in 4.4 mM $MgCl_2$ for 12 h before data collection (high-[Mg^{2+}] crystals).

Data Collection. Diffraction data were collected at 4 °C with graphite-monochromated Cu Kα X-rays from a Rigaku RU-200 rotating anode diffractometer at the UCSD Research Resource equipped with two Xuong–Hamlin multiwire area detectors (Hamlin et al., 1981; Xuong et al., 1985b). Data reductions were done using the UCSD area detector processing programs (Howard et al., 1985; Xuong et al., 1985a). $R_{sym} = \sum|I_{obsd} - I_{av}|/\sum I_{av}$ and data statistics are shown in Table I for both low- and high-[Mg^{2+}] crystals.

Refinement. The initial difference Fourier map, calculated using the refined 2.7-Å binary model phases and ternary complex diffraction data, showed the general location of the nucleotide binding site (Knighton et al., 1991a). In that map, the positions of the adenine ring, the ribose, and the α-phosphate were clearly recognizable, but the locations of the β- and γ-phosphates and Mg^{2+} were unclear. In an effort to better define the phosphate moieties, the crystals, grown under conditions to low-[Mg^{2+}] relative to ATP, were also soaked in a high-[Mg^{2+}] solution.

During model preparation, a polypeptide register error, confirmed by high-resolution refinement of the binary C:PKI-(5-24) structure (D. R. Knighton and R. Karlsson, personal communication) was found for residues 55–64 and 309–339 of the published binary structure (Knighton et al., 1991a). These changes did not alter any of the consensus residues described previously, and these revised coordinates are now available from the Brookhaven Data Bank as 2CPK.

Table II: Refinement Results

model	refinement	
	X-PLOR	TNT
enzyme 15–350	2.7–10 Å	2.7–20 Å
PKI(5–24)	11 552 reflns	11 773 reflns
2 Mg^{2+}, 1 ATP,	rms (Δ bond) = 0.021 Å	rms (Δ bond) = 0.018 Å
1 H_2O	rms (Δ angle) = 3.9°	rms (Δ angle) = 3.1°
fixed B = 17 Å^2	R^a = 0.212	R = 0.224
total 2972 atoms		

[a] R factor is defined as $\sum|F_o - F_c|/\sum F_o$.

The ternary complex model was refined with X-PLOR (Brunger et al., 1990; Brunger et al., 1987) using simulated annealing (SA) and conjugate gradient positional refinement. A slow-cooling SA protocol (Brunger et al., 1990) was used with a starting temperature of 4000 K and a final temperature of 300 K. For each of 148 temperature decrements, 0.5-fs steps of molecular dynamics were executed. Prior to simulated annealing, 40 cycles of conjugate gradient energy minimization were executed, and at this stage, all temperature factors and all occupancies were set at 17 Å^2 and 1.0, respectively. Charges of Lys, Arg, Asp, and Glu side chains were also set to zero. After simulated annealing, 120 cycles of conjugate gradient energy minimization were executed (see Table II). After each round of refinement, the regions of interest were inspected. ATP, two Mg^{2+} ions, one H_2O molecule, and residues adjacent to the ATP binding site were built into difference maps prepared from model phases after refinement of a model omitting atoms from any volume under consideration. Additional positional refinement was carried out with TNT (Tronrud et al., 1987) as a control in order to improve the geometry. X-PLOR refinement and R factor ($\sum|F_o - F_c|/\sum F_o$) calculations used $F/\sigma > 2$ data; TNT refinement and R factor calculations used $F/\sigma > 0$ data.

RESULTS

A model of this high-[Mg^{2+}]ternary complex was refined using X-PLOR to an R factor of 0.212 against 2.7–10 Å data with all atoms at B = 17 Å^2 (Table II). The model has rms deviations from ideal bond lengths and angles of 0.021 Å and 3.9°. Refinement of this model by TNT resulted in an overall R = 0.224 for data from 2.7 to 20 Å and gave rms deviations from ideal bond lengths and angles of 0.018 Å and 3.1°. All residues are within allowed (φ,ψ) regions in a Ramachandran plot. The difference Fourier maps for both the low- and high-[Mg^{2+}] crystals are shown in Figure 1. The difference Fourier map, calculated using phases derived from the final model, shows ATP and two Mg^{2+} metal sites. In order to independently confirm the two metal binding sites, the ternary complex crystals were soaked in high [Mn^{2+}] under conditions identical to those described for high [Mg^{2+}]. An anomalous Fourier synthesis using refined phases of the ternary complex and data from 4 to 10 Å of these high-[Mn^{2+}] ternary complex crystals showed, unambiguously, the presence of the two largest peaks coinciding with the positions of two Mg^{2+} metal sites (data not shown).

The ternary complex crystallizes in space group $P2_12_12_1$ with unit cell parameters a = 73.70 Å, b = 76.26 Å, and c = 80.74 Å. These dimensions differ by less than 0.5% along any axis from those of the binary complex. When the binary and ternary complexes were compared, least-squares superposition the the Cα atoms of both complexes showed an rms deviation of 0.55 Å, indicating that the refined ternary complex model has a conformation similar to that of the binary complex.

FIGURE 1: Stereoviews of electron density difference Fourier maps showing the position of MgATP in the ternary complex. Two 2.7–10 Å ($F_o - F_c$) difference maps were contoured at 3.0-σ positive density levels. Both maps were calculated using phases derived from the TNT refined model. MgATP was omitted in the F_c and phase calculation. In map A (top), the high-[Mg^{2+}] crystal diffraction data (F_o) were used. The difference Fourier map shows clearly two metal sites and one solvent molecule. ATP is shown in black; Mg^{2+} ions and solvent are indicated by black crosses. In map B (bottom), the low-[Mg^{2+}] crystal diffraction data (F_o) were used. The map was contoured at the same σ level as the high-[Mg^{2+}] crystal difference Fourier map.

This is consistent with earlier predictions based on low-angle neutron scattering, indicating that peptide, not MgATP, induces the major conformational changes (Parello et al., 1992).

MgATP is deeply buried, sandwiched between the small and large lobes and masked as well by the peptide and by the C-terminal region of the polypeptide chain. Before the details of the MgATP binding site are discussed, the general shielding of MgATP from solvent should be emphasized. The C-terminal tail (residues 300–350) wraps around the surface of the enzyme covering both lobes. This segment lies outside the core shared by all protein kinases. The segment that passes through the linker region that joins the two lobes is particularly noteworthy because it contains a patch of acidic residues (D^{328}-DYEEEE). Several of these residues come close to the P-3 Arg in the inhibitor peptide and probably contribute to peptide recognition. The others, while they do not interact directly with the nucleotide, nevertheless do shield the nucleotide from the solvent. These carboxyl groups are also very reactive with 1-ethyl-3-[3-(dimethylamino)propyl]carbodiimide hydrochloride (EDC) in the free C subunit, but are partially protected in the presence of MgATP and protected nearly completely in the ternary complex (Buechler & Taylor, 1990). On the basis of the chemical results alone this seems to be a region that is particularly sensitive to conformational changes. The shielding of the nucleotide provided by this C-terminal segment is seen clearly in Figure 2. This region clearly has implications for potential differences in nucleotide specificity between members of the protein kinase family, since in some cases, such as cdc2, an extension at the C-terminus does not exist (Hanks et al., 1988) and in other cases, such as MLCK (Knighton et al., 1992), the C-terminus interacts with other regions of the protein.

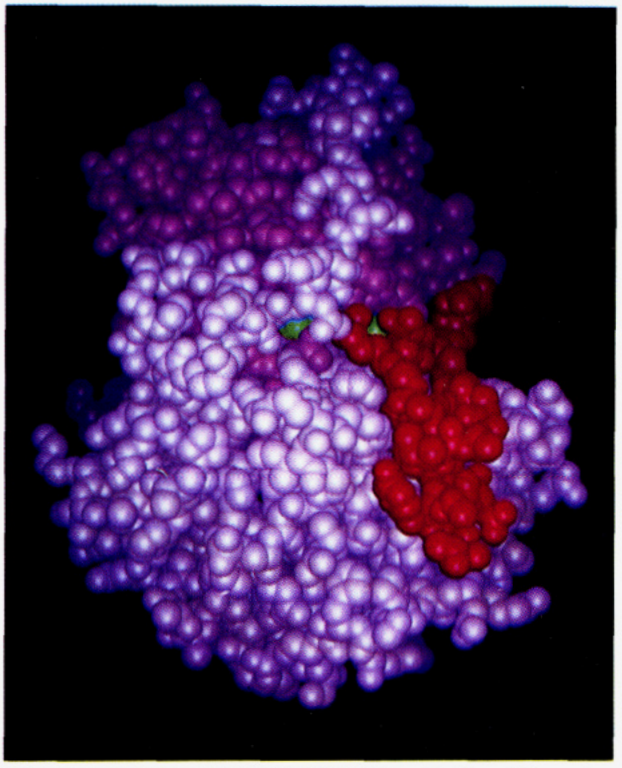

FIGURE 2: Space-filling model of the ternary complex. The amino-terminal region (residues 15–127) is shown in dark purple with the rest of the polypeptide chain shown in light purple. The buried ATP is shown in green and PKI(5-24) in red.

Description of the ATP Binding Site. (A) Adenine Ring. The adenine ring is enclosed in a hydrophobic pocket formed at the domain interface and consists of residues Leu49, Val57,

Ala70, Met120, Tyr122, and Val123 from the smaller, NH_2-terminal lobe and Leu173 from the larger, COOH-terminal lobe. The hydrophobic character of these residues is conserved within the protein kinase family. Two hydrogen bonds serve to anchor the adenine ring in this hydrophobic pocket. The primary hydrogen bond contact is between the N6 amino group and the main-chain carbonyl of Glu121 (Figure 3A). This hydrogen bonding to the N6 amino group is also very consistent with prior analog studies (Flockhart et al., 1984; Hoppe et al., 1978; Leonard et al., 1978) since the removal of a hydrogen bond donor at this position is very deleterious. For example, when the N6 amino group is replaced by a hydroxyl group and tautomerizes to the ketone form, it loses its hydrogen-bond-forming ability and a dramatic decrease in binding affinity is seen (Hoppe et al., 1978; taylor et al., 1990a). Hence, this small segment (Met120 through Val123) that links β-strand 5 in the small domain with the D helix in the large domain, plays an important role in recognition of the adenine ring both by hydrophobic interactions and by hydrogen bonding. In the conserved core shared by all members of the protein kinase family, this is the single strand that links the two domains. A second hydrogen bond can form between the N7 nitrogen and the side-chain hydroxyl of Thr183. Thr183, however, is not conserved in other protein kinases.

(*B*) *Ribose Ring.* The ribose adopts a 3′-endo pucker with an anti-glycosidic angle $\chi = 47°$ between the adenine and ribose rings. While the adenine ring is held by interactions with the enzyme only, as seen in Figure 3A, the ribose ring interacts with both the enzyme and the inhibitor, PKI(5-24). Two primary interactions involve hydrogen bonding to the 2′- and 3′-OHs. The oxygen of the 2′-OH is located 2.6 Å from the side chain of Glu127. The 3′-OH is 2.8 Å from the NH1 in the P-3 arginine of PKI(5-24) and 2.6 Å from the α-carbonyl oxygen of Glu170. Analog studies indicate that substitutions on the ribose ring may have different consequences for the free C subunit as opposed to the type I holoenzyme where MgATP binds with a high affinity (Flockhart et al., 1984; Hoppe et al., 1978). Removal of the 2′-OH increased both the K_m(MgATP) for catalysis and the K_d(MgATP) for binding to the type I holoenzyme. In contrast, removal of the 3′-OH actually decreased the K_m(MgATP) nearly 10-fold while the K_d for high-affinity binding to the holoenzyme was increased. The C:PKI complex, like the type I holoenzyme, also binds MgATP with a high affinity (Whitehouse & Walsh, 1983).

(*C*) *Phosphates.* The phosphates of ATP interact with several invariant residues drawn from both domains of the enzyme (Figure 3B). Two invariant residues, Lys72 in β-strand 3 and Glu91 in α-helix C, hold the α-phosphate firmly in position. The side chain of Lys72 is 3.4 Å from the nearest oxygen of the α-phosphate and 3.2 Å from the β-phosphate. The side chain of Glu91, being 3.0 Å away from the side chain of Lys72, serves to stabilize these interactions of the Lys with the α- and β-phosphate. The β-phosphate, in addition, is held by interactions with the backbone amides of Gly55, Phe54, and possibly Ser53.

The catalytic loop (residues 166–171), an essential part of the large domain, provides several additional invariant amino acids that interact with the γ-phosphate and help to facilitate catalysis. The side chain of Lys168 is conserved in all kinases that transfer phosphate to Ser or Thr and in this inhibitor complex is only 3.1 Å from the γ-phosphate. Thus, the small domain fixes the nontransferable α- and β-phosphates, while the catalytic loop of the large domain is close to the γ-phosphate and positioned to facilitate catalysis. The side chain of Asn171 is 2.3 Å from the second metal site. The side chain of this invariant residue is also within hydrogen-bonding distance (2.7 Å) of the α-carbonyl oxygen of Asp166, so that this key catalytic loop of the protein kinase family is structurally constrained. The side chain of the invariant Asp166, also in the catalytic loop, is 3.7 Å from the Cβ of the P-position Ala in PKI(5-24). In a substrate, a hydroxyl group would be at this site to serve as the phosphate acceptor.

The major Mg^{2+} ion is coordinated by oxygens of the γ- and β-phosphates of ATP and by the invariant Asp184 (Figure 3C). In the current model, its coordination geometry does not resemble the typical octahedral ligand coordination, but there are some unidentified electron densities nearby that could represent solvent ligands. A second metal site was seen clearly when the crystals were soaked in a solution containing 10-fold higher (4.4 mM) magnesium, although it was also visible in the low-[Mg^{2+}] crystals. The Mg^{2+} at this second site is coordinated by the oxygens of the α- and γ-phosphates and by the side chain of Asn171.

The Protein Kinase Nucleotide Binding Motif. The unique nucleotide binding motif of cAPK is seen in Figure 4. Of the 11 nearly invariant residues in the protein kinase family, 8 are associated directly with nucleotide binding. Nearly all of the nucleotide binding motif is contained within the small lobe. A dominant feature of this lobe is the five-stranded antiparallel β-sheet which encompasses two sequence hallmarks of the protein kinase family: the glycine-rich loop *Gly*^{50}Thr-*Gly*SerPhe*Gly* between β-strands 1 and 2 and the invariant residue, Lys72, in β-strand 3. The C helix between β-strands 3 and 4 provides an additional invariant residue, Glu91, that ion-pairs with Lys72.

The primary function of this small lobe is to firmly anchor the nucleotide and the nontransferable phosphates. It does so by locking the adenine base securely into a buried hydrophobic pocket, by anchoring the β-phosphate via hydrogen bonding to backbone amides in the glycine-rich loop, and by anchoring the α-phosphate through an ion pair to Lys72 which, in turn, pairs with Glu91. This lysine does not correspond, either in its position or in its function, to Lys17 in p21^{ras} and Lys21 in porcine cytosolic adenylate kinase, the residues that are an essential part of the so-called "P-loop" (Saraste et al., 1990). Only two invariant residues from the large lobe contribute to nucleotide binding. Asp184 chelates the primary Mg^{2+} ion that bridges the β- and γ-phosphates, and Asn171 chelates the second Mg^{2+} ion. An additional residue from the large lobe, Lys168, is conserved in Ser/Thr kinases. It binds to the γ-phosphate in the inhibitor complex.

Interacting Loops at the Active Site. The relationship between the three key loops in the structure of the C subunit of cAPK is presented in Figure 5. The nucleotide binding domain holds the ATP molecule on one side of the cleft, while the catalytic loop containing Asn171, Lys168, and Asp166 embraces ATP from the other side of the cleft. A third loop between β-strands 8 and 9 contains the invariant Asp184. Asp184 and Lys168 are the two protein side chains that bridge the loops in the large lobe with the loop in the small lobe by providing an essential ligand for the catalytic metal ion and by helping to orient the γ-phosphate moiety. This may be analogous to the D-X-G motif found in actin and HSP70 (Flaherty et al., 1991), although the Asp to metal distance is different (5 Å in actin and HSP70). Therefore, three essential loops, the glycine-rich loop, the catalytic loop, and the D-F-G loop, come together at the active site to position the phosphates of MgATP so that the γ-phosphate is poised for rapid transfer to the protein substrate.

DISCUSSION

Much information regarding the ATP binding site of the C subunit was deduced prior to the structure solution, and

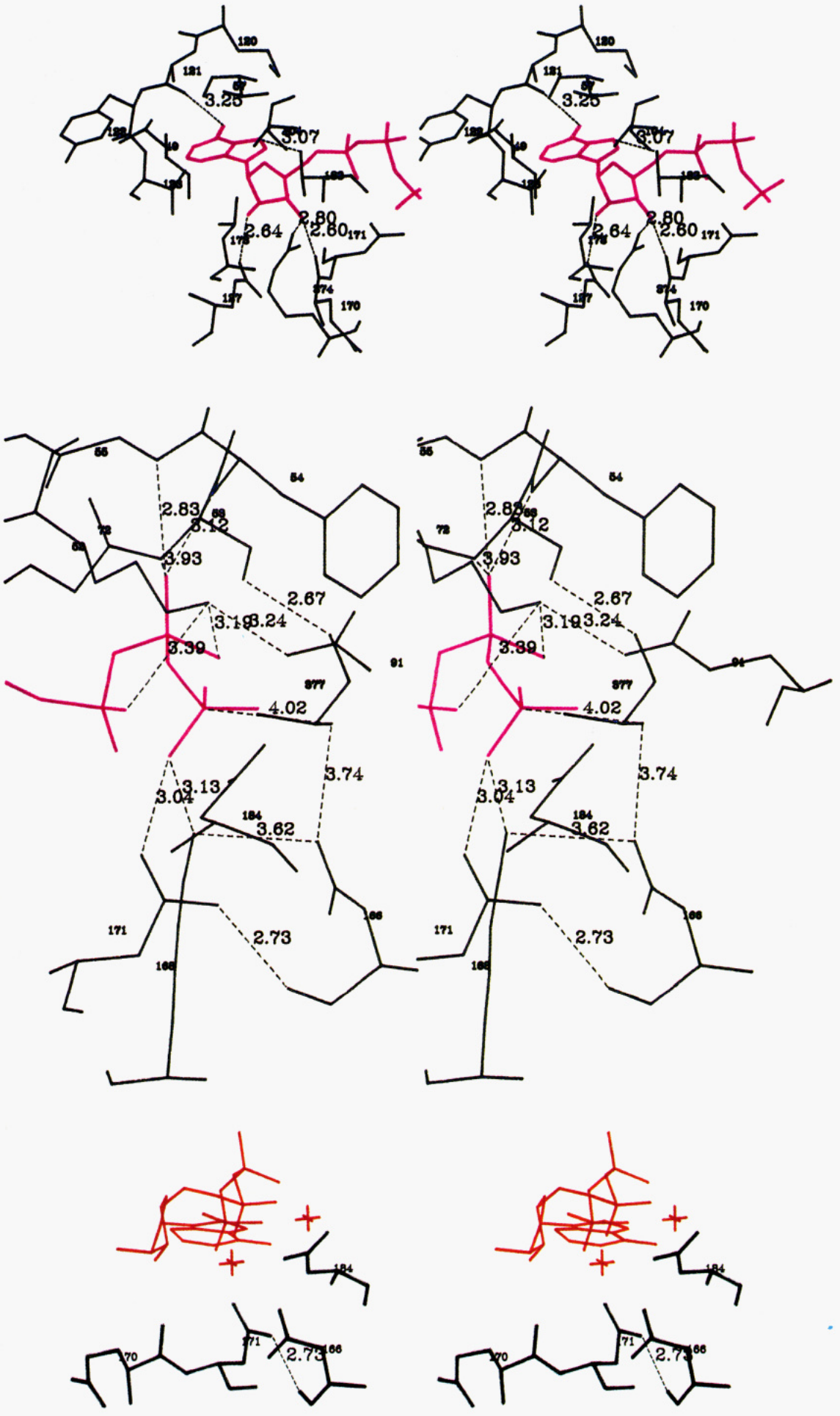
120
121
3.25
3.07
2.80
2.64
2.60
171
174
170
56
54
2.83
3.12
3.93
2.67
3.19
3.24
3.39
91
177
4.02
3.74
3.13
3.04
184
3.62
171
166
2.73
70

FIGURE 3: Structural features of the ATP binding site. (A, top) Adenosine binding pocket. A hydrogen bond between the N6 amino group of ATP and the main-chain carbonyl oxygen of Glu121 is indicated by a dashed line with a distance of 3.3 Å (3.25 Å). A second hydrogen bond between the N7 of ATP and the side chain of Thr183 is also shown. The side chain of Glu127 approaches the 2′-OH of the ribose at a distance of 2.6 Å (2.64 Å). The side chain of the P-3 arginine of PKI(5-24) and the main-chain carbonyl of Glu170 are 2.8 (2.80) and 2.6 Å (2.60 Å), respectively, away from the ribose 3′-OH. (B, middle) Phosphate binding region. The ATP phosphate region is shown in red while protein residues are shown in black. The glycine-rich loop interacts with the β-phosphate oxygen through the main-chain amides of the loop; the distances from amides to the β-phosphate oxygen are shown by dashed lines. The interactions between Lys72, the α- and β-phosphates, and residues in the vicinity of the γ-phosphate are also shown by dashed lines with labeled distances. (C, bottom) Structural features of the metal binding sites. ATP is shown in red while protein residues interacting with the metal ions are shown in black. The major metal site, coordinated by Asp184 and the β- and γ-phosphates, is indicated by a red cross. The minor metal binding site, coordinated by Asn171 and the α- and γ-phosphates, is also indicated by a red cross. A hydrogen bond is shown between the side-chain Asn171 and the carbonyl oxygen of Asp166, 2.7 Å (2.73 Å).

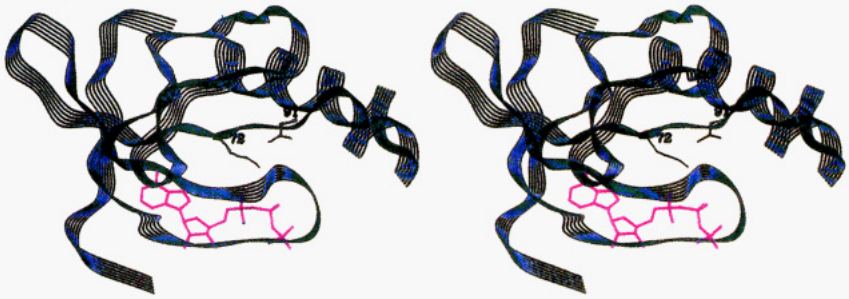

FIGURE 4: ATP binding motif. A stereoview of the ribbon drawing of the small domain extending from residue 40 (starting from top) through residue 127 (ending at lower part) shows a unique nucleotide binding motif of cAMP-dependent protein kinase. Side chains of Lys72 (β-strand 3) and Glu91 (helix C) are shown. Two antiparallel strands (β1,β2) hold the adenine ring, while the glycine-rich loop connecting β-strands 1 and 2 helps to fix the α- and β-phosphates.

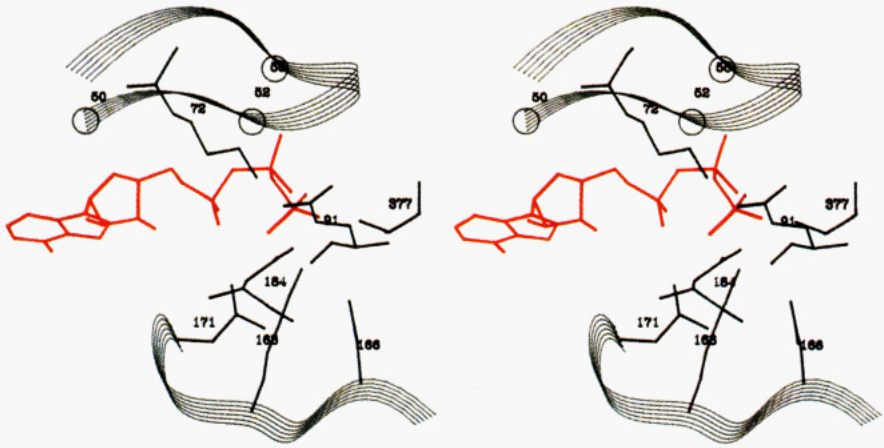

FIGURE 5: Relationship of the glycine loop and the catalytic loop. The Cα backbone of the glycine-rich loop (residues 50–58) is shown above ATP. The catalytic loop (residues 165–171), located underneath ATP, is shown with side chains of Asp166, Lys168, and Asn171. Lys72, Glu91, Asp184, and the inhibitor P-site residue Ala377 are shown approaching the γ-phosphate of ATP.

this information now can be correlated with the structure. The modification of Lys72 by affinity labeling with fluorosulfonyl benzoyl adenosine is fully consistent with the structure as is its proximity to Asp184 and Glu91 (Zoller et al., 1981). Lys72 interacts with the α- and possibly the β-phosphate of ATP, and the ε-NH_2 of Lys72 is anchored on the other side by the side chain of Glu91. The Asp184 that cross-links to Lys72 in the presence of DCCD chelates the major Mg^{2+} ion that bridges the β- and γ-phosphates. The fact that all three residues are invariant throughout the protein kinase family (Hanks, 1991) further attests to the essential role that each plays.

The predictions based on nucleotide analogs are consistent with a confined hydrophobic pocket for the adenine ring with strict steric constraints and a requirement for a small hydrogen bond donor at the N6 position. Analogs also demonstrated the importance of the phosphate moieties. At this point some of the unique features of the C subunit:PKI complex with respect to ATP binding should be emphasized (Taylor et al., 1990b; Walsh et al., 1990). PKI contains a pseudo substrate inhibitor site that occupies the consensus site portion of the substrate binding site. The K_m and K_d for MgATP interacting with the free C subunit are approximately 10 μM (Bhatnagar et al., 1983). In contrast, when the C subunit is complexed with PKI, MgATP binds with a high affinity (10–20 nM) (Whitehouse & Walsh, 1983). Furthermore, the high-affinity binding of PKI and MgATP is synergistic. Neither binds with a high affinity in the absence of the other. AMPPNP does not mimic ATP and fails to promote high-affinity binding of PKI (Whitehouse & Walsh, 1983). These results emphasize that the stereochemistry of the phosphate binding site is critical and that this inhibitory complex may differ somewhat from the catalytically competent complex of the enzyme with its substrate.

Some characteristic features of the phosphate binding sites emerged from the analog studies, and these, too, are consistent with the structure. First, MgATP and MgADP bind with equal affinity to the free C subunit (10 μM) (Bhatnagar et al., 1983). Second, neither Mg^{2+} nor ATP binds well alone (Armstrong et al., 1979). In contrast to ADP and ATP, AMP does not bind as a Mg^{2+} complex and has a very low affinity (K_i = 500 μM). Presumably, this is due to significant charge repulsion with Asp184 which would no longer be able to chelate a Mg^{2+}. Adenosine, however, binds well (K_i = 30 μM) indicating that, although activity is very sensitive to the phosphate moieties, the primary energy for binding comes

from the nucleotide. A fluorescence displacement method using *lin*-benzo-ADP showed that large bulky groups such as a tosyl moiety could be tolerated at the α-phosphate position, but not a negative charge (Bhatnagar et al., 1983).

The yeast catalytic subunit was probed by charge-to-alanine scanning mutagenesis where all charged residues were selectively changed to Ala (Gibbs & Zoller, 1991). Of the resulting mutants, only nine showed a greater than 95% decrease in specific activity, and all of these correlate with either conserved residues at the active site or with sites important for peptide recognition. Mutations of Lys72 and Glu91 in the small lobe caused an increase in K_m of up to 5-fold but produced an even greater increase in the K_m for the peptide. Only one mutant, the equivalent of Asp184Ala, was totally inviable in the yeast screen. The enzymes showing the greatest loss in k_{cat} (approximately 1000-fold) were the equivalents of Lys72Ala and Asp166Ala, while the equivalents of Lys168Ala and Arg280Ala caused a 50-fold decrease in k_{cat}. These mutations were characterized prior to the structure solution and are remarkably consistent with the structure.

Armstrong et al. (1979), using NMR spectroscopy and kinetic studies of inert ATP complexes, demonstrated that the Δ isomer of β,γ-bidentate $Co^{3+}(NH_3)_4ATP$ is the preferred isomer for the C subunit. This is consistent with what is observed in the crystal structure, although the angle between the adenine and the ribose ring is different. They showed, furthermore, that the C subunit binds one molecule of ATP and two metal ions. Occupancy of the second metal site is inhibitory when Mn^{2+} is the cation. The major metal site, occupied by Co^{3+} in their studies and coordinated by the oxygens of the β- and γ-phosphate, had a 10 times higher affinity than the minor site occupied by Mn^{2+} and coordinated to the oxygens of the α-, β-, and γ-phosphates. Binding of the minor site metal, furthermore, had no significant effect on the coordination of the major site.

The NMR results show good overall agreement with the crystal structure with regard to the number of metal sites and their interaction with ATP as well as overall stereochemistry (Bolen et al., 1980; Kaiser et al., 1981; Merritt et al., 1978). The crystals, grown under low-$[Mg^{2+}]$ conditions (Mg:ATP = 1:4) where ATP is in excess, identify the major Mg^{2+} site as the one bridging the β- and γ-phosphates and chelating with Asp184. High occupancy of the second site was achieved only when the crystals were soaked in high $[Mg^{2+}]$ (Mg:ATP = 2.5:1). This site bridging the α- and γ-phosphates is thus deduced to be the minor site. Armstrong et al. propose no direct protein ligand to the major metal binding site (Granot et al., 1980; Kaiser et al., 1981; Rosevear et al., 1984), while the X-ray structure unambiguously shows that the invariant Asp184 is a ligand to the major Mg^{2+} ion. These differences in the protein ligand assignment in the NMR and X-ray structures can be accounted for by the coordination sphere of the inert $Co^{3+}(NH_3)_4ATP$ complex utilized in the NMR studies. Four NH_3 groups chelating a Co^{3+} ion could easily prevent proper ligation by Asp184. This is supported by a decrease of 3 orders of magnitude in the activity of the enzyme complexed with $Co^{3+}(NH_3)_4ATP$. The coordination sphere of the inert $Co^{3+}(NH_3)_4ATP$ might also account for the observed differences in the intermetallic distances in the two structures (Granot et al., 1980; Rosevear et al., 1984). The most significant differences between NMR and X-ray data, however, are found in the network of distances between the peptide substrate or inhibitor and the γ-phosphate. NMR results based on complexes with a poor inhibitor, L-R-R-A-A-L-G (K_i = 490 μM), and a good substrate, L-R-R-A-S-L-G (K_m = 16 μM) (Kemp et al., 1977), show larger distances than those observed in the X-ray structure of the catalytic subunit complexed with a potent inhibitor, PKI(5-24) (K_i = 2.3 nM). For example, Granot et al. (1980) and Rosevear et al. (1984) reported distances of 5.3 Å from the γ-phosphate of ATP to the serine hydroxyl and 8.1 Å from the Cβ of serine to the major metal site. In the crystal structure, the distance from the Cβ of Ala377 at the P-site to the γ-phosphate of MgATP is only 4.2 Å, while the distance to the major Mg^{2+} site is only 4.7 Å. Thus, whereas the NMR data favored a dissociative mechanism, the crystallographic evidence is consistent with an associative mechanism.

On the basis of kinetic evidence, occupancy of a second metal site by Mn^{2+} is inhibitory; however, the situation with Mg^{2+} is different. Two Mg^{2+} ions are associated with binding of both ADP and ATP under physiological conditions (Granot et al., 1980). The occupancy of the second site causes a decrease in K_m (ATP) of approximately 10-fold depending on the salt concentration (Cook et al., 1982), and the crystal structure explains this enhanced affinity. A decrease in V_{max} is also observed with high $[Mg^{2+}]$. This effect on V_{max} is very likely due to the enhanced binding of MgADP, the release of which is the rate-limiting step in the reaction (Adams & Taylor, 1992).

Clearly, additional structures are required where both the metal and nucleotide are varied in order to understand the details of the region flanking the γ-phosphate and how this differs in an inhibitor complex as opposed to a catalytically competent complex.

Catalytic Mechanism. Correlation of previous kinetic studies with the crystal structure unambiguously establishes the stereochemistry of the phospho transfer reaction. Ho et al. (1988) demonstrated that phosphoryl transfer proceeds with an inversion of configuration at the phosphorus. The distances discussed above between the γ-phosphate and the P-site residue are also consistent with a direct in-line transfer involving a pentacovalent phosphate intermediate. A direct nucleophilic attack by the serine of the substrate is the most likely mechanism.

The requirement for a base catalyst at the site of phospho transfer is fulfilled by Asp166. It is the closest active site residue to Ala377 (3.7 Å) and is invariant in all protein kinases. The pH dependency of the catalytic reaction indicated that a residue having a pK_a of 6.2 was required for catalysis, and this was cited as evidence for a catalytic base (Yoon & Cook, 1987). Although recent studies (Adams & Taylor, 1992 (submitted); Yoon & Cook, 1987) indicate that the pK_a at 6.2 may not be due to a base catalyst at the active site as predicted, the structure is, nevertheless, consistent with a general-base-catalysis mechanism.

Another requirement is that the negative charges on the nucleotide be neutralized in order to facilitate the transfer. This is accomplished by the two Mg^{2+} ions, by two positively charged protein side chains, Lys72 and Lys168, and by the amides of the glycine-rich loop. The primary Mg^{2+} ion bridges the β- and γ-phosphates, and the Mg^{2+} in turn is also oriented by the side chain of Asp184. The charge is further neutralized by the binding of the second Mg^{2+} that bridges the α- and γ-phosphates. Several protein residues chelate this second Mg^{2+} ion. Two positively charged side chains, Lys72 and Lys168, bind to the phosphates of ATP. Their role is probably 2-fold; the first is to further neutralize the charges of the phosphates, and the second is to ensure proper stereochemistry. Lys168 lies close to the γ-phosphate (3.2 Å) in this inhibitor complex. If it occupies a similar position in a catalytically compentent complex, it could obviously participate in the phosphoryl transfer reaction. However, Lys168 could also

contribute to the high-affinity binding of MgATP in this complex. Unlike most lysine side chains in the C subunit, Lys168 does not react with acetic anhydride in the free enzyme, in the binary (C:MgATP) complex, or in the ternary complex (C:MgATP:PKI(5-24) (Buechler et al., 1989). Its lack of reactivity in the ternary complex is explained by the structure, but its lack of reactivity in the free C subunit has yet to be explained. Lys168 is conserved among Ser/Thr protein kinases, but is absent in the tyrosine kinases.

Although additional structures of complexes containing a bound substrate rather than an inhibitor will be required to better understand the mechanism, the clustering of conserved residues at the active site (Figure 5) is consistent with a direct nucleophilic attack of the serine oxygen on the γ-phosphate. The interactions of these residues with both MgATP and substrate provide a clear picture of how the protein contributes to the stereochemical alignment of the substrates and how potential transition-state intermediates might be stabilized. Once substrate and MgATP are bound, catalysis occurs rapidly. The off-rate for the phosphopeptide is fast, and the rate-limiting step is the release of MgADP (Adams & Taylor, 1992; Cook et al., 1982).

ACKNOWLEDGMENT

We thank the following individuals and resources for their contributions: Sean Bell for technical assistance; the NIH National Research Resource at UCSD (RR01644) and staff members Chris Nielsen and Don Sullivan for access to data collection facilities; the San Diego Supercomputer Center for use of the Advanced Scientific Visualization Laboratory and the Cray Y-MP8/864; and, in particular, Drs. Joseph Adams, Friedrich Herberg, and Bryan Driscoll for helpful discussion during the preparation of this manuscript.

REFERENCES

Adams, J. A., & Taylor, S. S. (1992) *Biochemistry 31*, 8516–8522.

Adams, J. A., & Taylor, S. S. (1992) *J. Biol. Chem.* (submitted for publication).

Armstrong, R. N., Kondo, H., Granot, J., Kaiser, E. T., & Mildvan, A. S. (1979) *Biochemistry 18*, 1230–1238.

Bhatnagar, D., Roskoski, R. J., Rosendahl, M. S., & Leonard, N. J. (1983) *Biochemistry 22*, 6310–6317.

Bolen, D. W., Stingelin, J., Bramson, H. N., & Kaiser, E. T. (1980) *Biochemistry 19*, 1176–1182.

Brunger, A. T., Krukowski, A., & Erickson, J. W. (1990) *Acta Crystallogr. A46*, 585–593.

Brunger, A. T., Kuriyan, J., & Karplus, M. (1987) *Science 235*, 458–460.

Buechler, J. A., & Taylor, S. S. (1988) *Biochemistry 27*, 7356–7361.

Buechler, J. A., & Taylor, S. S. (1989) *Biochemistry 28*, 2065–2070.

Buechler, J. A., & Taylor, S. S. (1990) *Biochemistry 29*, 1937–1943.

Buechler, J. A., Vedvick, T. A., & Taylor, S. S. (1989) *Biochemistry 28*, 3018–3024.

Cook, P. F., Neville, M. E., Vrana, K. E., Hartl, F. T., & Roskoski, J. R. (1982) *Biochemistry 21*, 5794–5799.

Flaherty, K. M., McKay, D. B., Kabsch, W., & Holmes, K. C. (1991) *Proc. Natl. Acad. Sci. U.S.A. 88*, 5041–5045.

Flockhart, D. A., Freist, W., Hoppe, J., Lincoln, T. M., & Corbin, J. D. (1984) *Eur. J. Biochem. 140*, 289–295.

Gibbs, C. S., & Zoller, M. J. (1991) *Biochemistry 30*, 5329–5334.

Granot, J., Mildvan, A. S., & Kaiser, E. T. (1980) *Arch. Biochem. Biophys. 205*, 1–17.

Hamlin, R., Cork, C., Niesen, C., Vernon, W., Matthews, D., & Xuong, N.-H. (1981) *J. Appl. Crystallogr. 14*, 85.

Hanks, S. K. (1991) *Curr. Biol. 1*, 369–383.

Hanks, S. K., Quinn, A. M., & Hunter, T. (1988) *Science 241*, 42–52.

Ho, M.-f., Bramson, H. N., Hansen, D. E., Knowles, J. R., & Kaiser, E. T. (1988) *J. Am. Chem. Soc. 110*, 2680–2681.

Hoppe, J., Freist, W., Marutzky, R., & Shaltiel, S. (1978) *Eur. J. Biochem. 90*, 427–432.

Howard, A. J., Nielson, C., & Xuong, N.-h. (1985) *Methods Enzymol. 14*, 452–472.

Kemp, B. E., Graves, D. J., Benjamini, E., & Krebs, E. G. (1977) *J. Biol. Chem. 252*, 4888–4894.

Knighton, D. R., Zheng, J., Ten Eyck, L. F., Ashford, V. A., Xuong, H.-h., Taylor, S. S., & Sowadski, J. M. (1991a) *Science 253*, 407–414.

Knighton, D. R., Zheng, J., Ten Eyck, L. F., Xuong, N.-h., Taylor, S. S., & Sowadski, J. M. (1991b) *Science 253*, 414–420.

Knighton, D. R., Pearson, R. B., Sowadski, J. M., Means, A. R., Ten Eyck, L. F., Taylor, S. S., & Kemp, B. E. (1992) *Science 258*, 130–135.

Leonard, N., Scopes, D. C. I., VanDerLijn, P., & Barrio, J. (1978) *Biochemistry 17*, 3677–3684.

Merritt, E., Sundaralinam, M., Cornelius, R., & Cleland, W. W. (1978) *Biochemistry 17*, 3274–3278.

Parello, J., Timmins, P. A., Sowadski, J. M., & Taylor, S. S. (1992) *J. Mol. Biol.* (in press).

Rosevear, P. R., Fry, D., Mildvan, A., Doughty, M., O'Brian, C., & Kaiser, E. T. (1984) *Biochemistry 23*, 3161–3173.

Saraste, M., Sibbald, P. R., & Wittinghofer, A. (1990) *Trends Biochem. Sci. 15*, 430–434.

Shoji, S., Titani, K., Demaille, J. G., & Fischer, E. H. (1979) *J. Biol. Chem. 254*, 6211–6214.

Slice, L. W., & Taylor, S. S. (1989) *J. Biol. Chem. 264*, 20940–20946.

Taylor, S. S., Buechler, J. A., & Knighton, D. R. (1990a) in *Peptides and Protein Phosphorylation* (Kemp, B. E., Ed.) pp 1–42, CRC Press, Inc., Boca Raton, FL.

Taylor, S. S., Buechler, J. A., & Yonemoto, W. (1990b) *Annu. Rev. Biochem. 59*, 971–1005.

Tronrud, D. E., Ten Eyck, L. F., & Matthews, B. W. (1987) *Acta Crystallogr. A43*, 489.

Walsh, D. A., Angelos, K. L., Van Patten, S. M., Glass, D. B., & Garetto, L. P. (1990) in *Peptides and Protein Phosphorylation* (Kemp, B. E., Ed.) pp 43–84, CRC Press, Inc., Boca Raton, FL.

Walsh, D. A., Perkins, J. P., & Krebs, E. G. (1968) *J. Biol. Chem. 243*, 3763–3765.

Whitehouse, S., & Walsh, D. A. (1983) *J. Biol. Chem. 258*, 3682–3692.

Xuong, N.-h., Nielsen, C., Hamlin, R., & Anderson, D. (1985a) *J. Appl. Crystallogr. 18*, 342–350.

Xuong, N.-h., Sullivan, D., Nielsen, C., & Hamlin, R. (1985b) *Acta Crystallogr. B41*, 267–269.

Yonemoto, W., McGlone, M. L., Slice, L. W., & Taylor, S. S. (1991) in *Protein Phosphorylation (Part A)* (Hunter, T. & Sefton, B. M., Eds.) pp 581–596, Academic Press, Inc., San Diego.

Yoon, M.-Y., & Cook, P. F. (1987) *Biochemistry 26*, 4118–4125.

Zheng, J., Knighton, D. R., Parello, J., Taylor, S. S., & Sowadski, J. M. (1991) in *Protein Phosphorylation (Part A)* (Hunter, T., & Sefton, B. M., Eds.) pp 508–521, Academic Press, Inc., San Diego.

Zheng, J., Knighton, D. R., Xuong, N.-h., Parello, J., Taylor, S. S., & Sowadski, J. M. (1992) *Acta Crystallogr. B48*, 241–244.

Zoller, M. J., Nelson, N. C., & Taylor, S. S. (1981) *J. Biol. Chem. 256*, 10837–10842.